

Supplemental information

Sipa1 Deficiency Induced Bone Marrow Niche Alterations Lead to the Initiation of Myeloproliferative Neoplasm

Pingnan Xiao¹, Monika Dolinska¹, Lakshmi Sandhow¹, Makoto Kondo¹, Anne-Sofie Johansson¹, Thibault Boudierlique¹, Ying Zhao², Xidan Li³, Marios Dimitriou¹, George Z. Rassidakis⁴, Eva Hellström Lindberg¹, Nagahiro Minato⁵, Julian Walfridsson¹, David T. Scadden⁶, Mikael Sigvardsson⁷, Hong Qian^{1*}

- Supplemental methods
- Figure legend S1-6;
- Table S1 and S2
- Supplemental Reference: 10
- Graphical abstract

Supplemental Methods

Isolation of mononuclear cells from mouse BM

This was done as previously described.¹ Briefly, femurs, tibias and iliac crest were crushed in PBS+10% FBS (PAA). The marrow cells were collected. The cells from bone were obtained by subsequent treatment of bone fragments with 0.1% Collagenase II (CLS II Worthington Biochemical) and 0.05% trypsin-EDTA for 30-45 min at 37°C. The bone and marrow cells were pooled and spun down at 300 g for 5-10 min and then resuspended in PBS+10% FBS for MSC isolation.

Multi-color fluorescence activated cell sorting (FACS) of MSCs

Mouse and human MSCs were isolated as described.² For mouse MSC isolation, the BM hematopoietic cells were first depleted by staining the cells with purified rat anti-mouse CD45 and hematopoietic lineage (LIN) markers TER119, B220 or CD19, CD4, CD8, GR1, CD11B and subsequently using sheep anti-rat Dynabeads (Invitrogen). The remaining hematopoietic cells were visualized by fluorescence-conjugated CD45 and TER119 for further removal of hematopoietic cells. Fluorochrome-conjugated antibodies CD31, SCA1, CD51 and CD44 were used for subfractionating the mesenchymal cells into CD45⁻LIN⁻CD44⁻CD51⁺SCA1⁺ MSCs, CD45⁻LIN⁻CD44⁻CD51⁺SCA1⁻ progenitors, CD45⁻LIN⁻CD44⁻CD51⁻SCA1⁻ mature cells and CD31⁺ endothelial cells. Dead cells were excluded by propidium iodine (PI) staining. The BM stromal cell subsets were sorted or analyzed on FACS Aria III (BD). The cells were gated according to fluorescence minus one (FMO) using cells. The human BM MSCs were isolated as described.² See Table S1 for detailed information about the antibodies used in the study.

***In vitro* differentiation assays**

The assays were performed as previously described.¹ The CD45⁻TER119⁻CD31⁻CD44⁻SCA⁺CD51⁺ cells were sorted and cultured for 7-10 days. The cells were then cultured in differentiation induction media for osteoblast, adipocyte and chondrocyte differentiation. The media were changed twice a week for 21-28 days. For osteoblast differentiation, the cells were cultured in complete osteogenic medium made by mixing Human/Mouse StemXVivo Osteogenic/Adipogenic Base Media (CCM007) and Mouse StemXVivo Osteogenic Supplement (CCM009, R&D System). At day 21-28 after induction, the cells were fixed with ice-cold methanol and stained with 1% Alizarin Red S (Sigma) (pH 4.1) for 5-10 min. The excess dye was removed and the wells were dehydrated, subsequently mounted with Clear MountTM Mounting solution (Invitrogen, CA, USA). For adipogenesis, the cells were cultured in DMEM GlutaMAX (Gibco) supplemented with 10% FBS, 10 mM HEPES, 100 U/mL penicillin, 100 µg/mL streptomycin, 5-10 µg/mL insulin (Sigma), 20 µM indomethacin (Sigma) or 0.5 mM isobutylmethylxanthine (Sigma), 1x10⁻⁶ M dexamethasone (Sigma). The cells were fixed with 10% formalin and stained with 0.5% Oil Red O (Sigma) in isopropanol (Sigma). The chondrocyte differentiation was induced in monolayer culture, the cells were cultured in a 96-well plate or 12-well plates in complete DMEM+high glucose 4.5 g/L containing 10⁻⁷ M dexamethasone, 1% ITS (Sigma), 2 mM sodium pyruvate (Sigma), 0.35 mM proline (Sigma) and 10 ng/ml TGF-β3 (R&D System). The chondrocyte differentiation was assessed by staining of proteoglycan with Toluidine blue (Sigma) (pH 2.0 to 2.5). Then removed the excess dye and washed three times with distilled water. The images were taken using a bright field microscope.

Analysis of hematopoietic cell transformation after transplantation

Peripheral blood (PB) samples were collected monthly from the tail vein in EDTA-coated tubes (Sarstedt) after transplantation for 9 months for analysis. PB was counted in an automated cell

counter (Sysmex) for different blood components. The blood cell morphology was analyzed by blood smears and cytopsin stained by May-Grünwald-Giemsa (Sigma). The PB mononuclear cells were isolated using 2% Dextran T-500 (Pharmacia, Uppsala, Sweden) and 0.8% Ammonium Chloride (Stem Cell Tech.). PB and BM myeloid lineage (CD11B⁺GR1⁺ and CD11B⁺GR1⁻ monocytes), B cell lineage (CD19⁺) and T cell lineage (CD4⁺ / CD8⁺ or CD3⁺) were analyzed within the CD45.1 or CD45.2 donor cells. At the end point (9 months or earlier) of the transplantation experiments, bones (femurs, tibiae and crest iliac), spleens and lymph nodes were also harvested from the recipient mice for FACS and histology analysis. HSC and progenitors were analyzed as described³. Briefly, BM MNCs were isolated and stained with anti-mouse CD16/32-PECY7, CD135-PE, lineage (LIN) cocktail CD3/GR1/TER119/CD11B/NK1.1-PECY5, CD117-APCCY7, CD34-FITC, CD150-APC and SCA1-Pacific Blue antibodies. All samples were stained with the vital marker PI prior to analysis on FACSDiva for FACS Fortessa LSR II (BD). LIN⁻SCA1⁺KIT⁺ (LSK), short-term (ST)-HSC (LSKCD34⁺FLT3⁻), long-term (LT)-HSC (LSKCD34⁻FLT3⁻CD150⁺), common myeloid progenitor (CMP, LIN⁻SCA1⁻KIT⁺CD34⁺FcγR^{low}), granulocyte-macrophage progenitor (GMP, LIN⁻SCA1⁻KIT⁺CD34^{high}FcγR^{high}) and MK-erythrocyte progenitor (MEP, LIN⁻SCA1⁻KIT⁺CD34⁻FcγR⁻) were defined as described.⁴ Data analysis was carried out with FlowJo software (TreeStar Inc.). See Table S1 for detailed information about the antibodies used in the study.

Quantitative RT-PCR

BM stromal subsets were sorted directly into RLT buffer (Qiagen) containing 2-Mercaptoethanol (143 mM, Sigma) and kept at -80 °C. RNA extraction and DNase treatment was performed with the RNeasy Micro Kit (Qiagen) according to the manufacturer's instructions for samples

containing less than 10^5 cells. Eluted RNA samples were reverse transcribed using SuperScript® III Reverse Transcriptase (Invitrogen, catalog number: 18080044), RNase OUT (ThermoFisher) and random primers (Invitrogen) according to protocol supplied by the manufacturer. Real-time quantitative PCR (Q-PCR) reactions were performed by mixing 2 x TaqMan universal PCR master mix, 20 x TaqMan primer/probe mix, RNase-free H₂O and 2 μ l of cDNA for a final reaction volume of 8 μ l in 384-well plates in CFX384 Touch™ Real-Time PCR Detection System. See Table S2 for the information about Assays-on-Demand probes.

RNA sequencing and data analysis

RNA from BM stromal cell subsets that were sorted from *Sipa1*^{-/-} and age-matched *Sipa1*^{+/+} mice was extracted using RNeasy microkit (Qiagen, USA) according to the manufacturer's recommendations. cDNA library was prepared by using the Ovation® Ultralow Library Systems (L2DR-BC1-16, NuGEN Technologies, San Carlos, CA) and subjected to 50 cycles of HiSeq 2000 or 76 cycles of NextSeq500 sequencing (Illumina, San Diego, CA) generating 20-30 million reads/sample.

All raw sequence reads available in FastQ format were mapped to the mouse genome (mm10) using Tophat2 combining with Bowtie2.^{5,6} PCR duplicates were removed using samtools⁷ after reads mapping. Next, raw reads mapped to each gene were calculated using FeatureCounts from Subread package.⁸ Genes with Reads Per Kilobase of transcript per Million mapped reads (RPKM) values more than 0.1 were considered as being actively transcribed and proceeded to the analysis of Differential Gene Expression (DGE).⁹ DEseq2 was used to perform the analysis of DGE, where genes with raw read counts as input. The differentially expressed genes were identified by adjust *P* value for multiple testing using Benjamini-Hochberg correction with False Discovery Rate (FDR) values less than 0.2.

The major computations were performed on resources provided by SNIC through Uppsala Multidisciplinary Center for Advanced Computational Science (UPPMAX) under Project b2014299.

For Gene set enrichment analysis (GSEA), the read counts were first normalized by the Trimmed mean of M-values normalization method (TMM),¹⁰ and then the normalized read counts were performed on the GSEA platform from Broad Institute (<http://www.broadinstitute.org/gsea/index.jsp>). The analyses were based on gene ontology (c5.all.v2.5.symbols.gmt), BioCarta (c2.biocarta.v2.5.symbols.gmt) and KEGG (c2.kegg.v2.5.symbols.gmt). Gene sets with a nominal *P* value < .05 and FDR < .25 were considered to be significantly enriched. Within each gene set, genes ranked in both the leftmost (indicates the strong positive correlation with *Sipal*^{-/-} phenotype) and rightmost (indicates the strong negative correlation with *Sipal*^{-/-} phenotype), were referred to contribute to the leading edges effect for the core enrichment.

Micro-Computed Tomography (CT)

Quantum FX μ CT (PerkinElmer, Waltham, MA, USA) is used for bone μ CT scan, with voltage at 90Kv, current at 160 μ A, Field of View at 20 or 5, scan time at 4.5 min. 3D μ CT image reconstruction was generated using Viewer (PerkinElmer, Massachusetts, USA) software. Bone segmentation and bone / bone marrow volume quantification were generated by Analyze 12.0 (AnalyzeDirect, KS, USA).

Histology analysis

Mouse bones were fixed in 4% paraformaldehyde (PFA), decalcified with 10% EDTA (Sigma) at pH7.2, dehydrated in increasing ethanol concentrations, cleared in xylene and then embedded

in paraffin. Mouse spleens were also fixed in 4% PFA and embedded in paraffin. Tissue sections (4- μ m thickness) were stained with Hematoxylin and eosin (HE). Blood smear and cytopsin slides were stained by May-Grünwald-Giemsa. HE images of bone sections were taken using 3D Histech Slide Scanner using Panoramic MIDI (3D HISTECH). Panoramic Viewer (3D HISTECH) was used for taking images of blood, BM, and spleen, and calculating megakaryocytes numbers per area.

***In vitro* co-culture experiments**

BM LSK hematopoietic stem and progenitor cells were sorted from 10-week old *Sipa1*^{+/+} mice and co-cultured with freshly sorted BM stromal subsets (MSCs, MPCs, CD51⁻SCA1⁻ cells, and CD31⁺ endothelial cells from 3-month old *Sipa1*^{+/+} and *Sipa1*^{-/-} mice in Myelocult (M5300 + 10⁻⁶ M hydrocortisone, Stem cell technology) at a density of 5000 LSK and 6000 stromal cells per well in a 96-well plate. The cells from each well were collected 2.5 days after co-culture and 2% of the total cells (equivalent to 100 LSK of input) transferred to Methocult M3434, Stem cell technology) in a petri dish for colony-forming units in culture (CFU-Cs). Colonies (>50 cells per colony) were scored as burst-forming unit- erythrocytes (BFU-E), CFU-granulocyte-macrophage (GM), and CFU-granulocytes (G) by morphology under microscope on day 8 after seeding. The E colonies were identified by 2,7-diaminofluorene (DAF, Sigma) staining at a working concentration of 0.5mg/ml (0.5 mL 10 mg/ml DAF in 90% glacial acetic acid, 0.1 mL 30% H₂O₂, and 10 mL 200 mM Tris-HCl, pH 7.5). The DAF-positive E colonies were identified as cells with intracellular blue granules. Cells were plated in duplicate for each assay.

Supplemental Figures

Figure S1. Development of the MPN in 16-month old *Sipa1*^{-/-} female mice. (A) Total WBCs in the aged *Sipa1*^{+/+} and *Sipa1*^{-/-} mice. n = 21 of *Sipa1*^{+/+}, n = 28 of *Sipa1*^{-/-} mice were included. (B) FACS analysis of lymphoid lineage cells in PB of the 16-month old mice. (C) Enhanced myelopoiesis was mainly observed in PB of 16-month old female mice. (D) Giemsa stained blood smear and isolated PB nucleated cells of 16-month old *Sipa1*^{+/+} and *Sipa1*^{-/-} mice. The red arrows indicate macrocytic red blood cells. The blue arrow indicates immature neutrophils. Scale bars represent 25 μ m. (E) Mean cell volumes (MCV) of PB of 16-month old *Sipa1*^{+/+} and *Sipa1*^{-/-} female mice. (F) One representative HE stained femoral section shows increased leukocytes infiltration in the *Sipa1*^{-/-} mice. Scale bars represent 500 μ m. The statistical difference was determined by Mann-Whitney (A-C) or unpaired *t* test (E). Related to Figure 2.

Figure S2. Normal hematopoiesis in young adult *Sipa1*^{-/-} mice. BM and PB were collected from 2-3 month old gender-matched *Sipa1*^{+/+} and *Sipa1*^{-/-} mice. (A) Similar counts of WBC, RBC, HGB and PLT in the *Sipa1*^{+/+} and *Sipa1*^{-/-} mice. (B) FACS analysis of hematopoietic cell lineages in PB of the *Sipa1*^{+/+} and *Sipa1*^{-/-} mice. (C) Total BM cellularity of the *Sipa1*^{+/+} and *Sipa1*^{-/-} mice. The cells were from two tibias and femurs of the mice (n = 13 and 15 for *Sipa1*^{+/+} and *Sipa1*^{-/-} mice respectively). (D) FACS profile showing gating strategy of BM hematopoietic stem and progenitor cells. (E) The frequencies of HSC and progenitor cells in BM MNCs of the *Sipa1*^{+/+} and *Sipa1*^{-/-} mice. (F) Histology of femoral bones from the *Sipa1*^{+/+} and *Sipa1*^{-/-} mice. Scale bars from left to right represent 1 mm, 500 μ m, 100 μ m, and 50 μ m, respectively. The statistical difference was determined by unpaired Mann-Whitney *t* test. Related to Figure 4.

Figure S3. Hematopoietic lineages in BM and hematopoietic progenitors in the recipient spleen 9 months after transplantation of normal hematopoietic cells into sublethally irradiated *Sipa1*^{+/+} and *Sipa1*^{-/-} recipient mice. (A) Donor derived BM engraftment 9 months after transplantation of CD45.1⁺ *Sipa1*^{+/+} cells. (B) BM lineage distribution of donor- and host-derived hematopoietic cells 9 months after transplantation of *Sipa1*^{+/+} hematopoietic cells into sublethally irradiated *Sipa1*^{+/+} and *Sipa1*^{-/-} recipient mice. (C) The enhanced expansion of donor (CD45.1⁺) -derived HSPCs and myeloid progenitors in the sublethally irradiated *Sipa1*^{+/+} and *Sipa1*^{-/-} spleen. (D) Host (CD45.2⁺)-derived HSPCs in the sublethally irradiated *Sipa1*^{+/+} and *Sipa1*^{-/-} recipient spleen. Statistical analysis was performed by unpaired Mann-Whitney test.

Related to Figure 5.

Figure S4. The development of MDS/MPN in the lethally irradiated *Sipa1*^{-/-} recipient mice. (A) Total engraftment of donor cells in the lethally irradiated *Sipa1*^{+/+} and *Sipa1*^{-/-} recipient mice after transplantation. (B) WBC, PLT RBC and HGB in the PB of the *Sipa1*^{+/+} and *Sipa1*^{-/-} mice at termination point post transplantation. The *P* values were determined by unpaired *t* test. (C) FACS analysis of PB lineages at termination time point after transplantation. (D) PB smears of the *Sipa1*^{+/+} and *Sipa1*^{-/-} mice 9 months after transplantation. The macrocytes are indicated by red arrows. Scale bars represent 25 μ m. (E) The enlarged lymph node in one of the *Sipa1*^{-/-} recipient mice after transplantation compared to that of *Sipa1*^{+/+} recipients. Related to Figure 6.

Figure S5. Dysregulated cytokine signaling pathways in the BM stromal cell subsets of *Sipa1*^{-/-} young mice. Gene-set enrichment analyses (GSEA) were carried out on the RNA

sequencing data to identify upregulated or downregulated Hallmark and KEGG terms in the *Sipa1*^{-/-} stromal cells. Data are from 3 independent sorting experiments. FDR-q value represents the false discovery rate of the *P* value. (A-B) Upregulated signaling pathways in the *Sipa1*^{-/-} MSCs (A) and endothelial cells (B). The G protein signaling and Kras signaling pathways are indicated by red arrows. (C) Downregulation of the oxidative phosphorylation gene sets and upregulation of Kegg_Fc_Epsilon_RI_signaling_pathway in the *Sipa1*^{-/-} MPCs. (D) Upregulated Il2, ECM-receptor and Wnt/ β catenin signaling pathways in the *Sipa1*^{-/-} endothelial cells. (E) The significant upregulated genes in the Wnt/ β catenin pathway in the *Sipa1*^{-/-} endothelial cells. Red indicates high expression and blue indicates low expression. Related to Figure 7.

Figure S6. KEGG pathway analysis shows the genes that are 2 fold upregulated in the Ras and Rap1 signaling pathways in the *Sipa1*^{-/-} MSCs. The analysis was performed on the RNA sequencing data using DAVID bioinformatics resources 6.8 (<https://david.ncifcrf.gov/summary.jsp>). The 2-fold upregulated genes were submitted to DAVID for mapping to KEGG (Kyoto Encyclopedia of Genes and Genomes) pathways. The upregulated genes in the Ras and Rap1 signaling pathways are indicated by red stars.

Related to Figure 7.

Table S1 Antibodies used for flow cytometry in the study

Antibody	Conjugate	Clone	Source
Anti-mouse TER-119	Purified	TER-119	Biolegend
Anti-mouse CD45	Purified	30-F11	Biolegend
Anti-mouse CD3	Purified	17A2	Biolegend
Anti-mouse/Human CD45R/B220	Purified	RA3-6B2	Biolegend
Anti-mouse Ly-6G/Ly-6C (Gr-1)	Purified	RB6-8C5	Biolegend
Anti-mouse CD19	Purified	6D5	Biolegend
Anti-mouse CD11B	Purified	M1/70	Biolegend
Anti-mouse CD16/32	Purified	93	Biolegend
Anti-mouse/Human CD44	APC/Cy7	IM7	Biolegend
Anti-mouse CD31	PE/Cy7	390	Biolegend
Anti-mouse CD45	PE/Cy5	30-F11	eBioscience
Anti-mouse TER-119	PE/Cy5	TER-119	Biolegend
Anti-mouse CD19	PE/Cy5	eBio1D3 (1D3)	eBioscience
Anti-mouse CD11b	PE/Cy5	M1/70	Biolegend
Anti-mouse CD51	PE	RMV-7	Biolegend
Anti-mouse Ly-6A/E (Sca-1)	Pacific Blue	D7	Biolegend
Anti-mouse CD4	APC	GK1.5	Biolegend
Anti-mouse CD8a	PE	53-6.7	Biolegend
Anti-mouse CD19	PE/Cy7	eBio1D3 (1D3)	eBioscience

Anti-mouse NK1.1	PE/Cy5	PK136	Biolegend
Anti-mouse/Human CD11b	APC/Cy7	M1/70	Biolegend
Anti-mouse Ly-6G/Ly-6C (Gr-1)	Brilliant Violet 421	RB6-8C5	Biolegend
Anti-mouse CD45.1	PerCP/Cy5.5	A20	Biolegend
Anti-mouse CD45.2	Alexa Fluor 700	104	Biolegend
Anti-mouse CD3e	PE/Cy5	145-2C11	Biolegend
Anti-mouse Ly-6G/Ly-6C (Gr-1)	PE/Cy5	RB6-8C5	Biolegend
Anti-mouse CD117	APC/Cy7	2B8	Biolegend
Anti-mouse CD16/32	PE/Cy7	93	eBioscience
Anti-mouse CD135	PE	A2F10	Biolegend
Anti-mouse CD34	FITC	RAM34	eBioscience
Anti-mouse CD45	MicroBeads	30F11.1	Miltenyi Biotec
Anti-human CD235A	eFluor 450	6A7M	eBioscience
Anti-human CD45	eFluor 450	HI30	eBioscience
Anti-human CD31	PE/CY7	WN59	Biolegend

Table S2 List of the probes used for Q-PCR.

Gene name	Assay ID	Full name
<i>Cxcl12</i>	Mm00445552_m1	C-X-C motif chemokine ligand 12
<i>Kitl</i>	Mm00442972_m1	Kit ligand

<i>Angptl1</i>	Mm00472259_m1	Angiopoietin-Like 1
<i>Il7</i>	Mm00434291_m1	Interleukin 7
<i>Runx2</i>	Mm00501584_m1	Runt related transcription factor 2
<i>Dicer1</i>	Mm00521722_m1	Dicer1, ribonuclease III
<i>Sipa1</i>	Mm00441411_m1	Signal-induced proliferation associated gene 1
<i>Hprt</i>	Mm01545399_m1	Hypoxanthine guanine phosphoribosyl transferase
<i>SIPA1</i>	Hs00534581_ml	Signal-induced proliferation associated gene 1
<i>HPRT</i>	Hs99999909_ml	Hypoxanthine guanine phosphoribosyl transferase

Supplemental References

1. Qian H, Badaloni A, Chiara F, et al. Molecular characterization of prospectively isolated multipotent mesenchymal progenitors provides new insight into the cellular identity of mesenchymal stem cells in mouse bone marrow. *Molecular and Cellular Biology*. 2013;33(4):661-677.
2. Qian H, Le Blanc K, Sigvardsson M. Primary mesenchymal stem and progenitor cells from bone marrow lack expression of CD44 protein. *The Journal of biological chemistry*. 2012;287(31):25795-25807.
3. Qian H, Buza-Vidas N, Hyland CD, et al. Critical role of thrombopoietin in maintaining adult quiescent hematopoietic stem cells. *Cell Stem Cell*. 2007;1(6):671-684.
4. Akashi K, Traver D, Miyamoto T, Weissman IL. A clonogenic common myeloid progenitor that gives rise to all myeloid lineages. *Nature*. 2000;404(6774):193-197.
5. Kim D, Pertea G, Trapnell C, Pimentel H, Kelley R, Salzberg SL. TopHat2: accurate alignment of transcriptomes in the presence of insertions, deletions and gene fusions. *Genome Biol*. 2013;14(4):R36.
6. Langmead B, Salzberg SL. Fast gapped-read alignment with Bowtie 2. *Nat Methods*. 2012;9(4):357-359.
7. Li H, Handsaker B, Wysoker A, et al. The Sequence Alignment/Map format and SAMtools. *Bioinformatics*. 2009;25(16):2078-2079.

8. Liao Y, Smyth GK, Shi W. featureCounts: an efficient general purpose program for assigning sequence reads to genomic features. *Bioinformatics*. 2014;30(7):923-930.
9. Mortazavi A, Williams BA, McCue K, Schaeffer L, Wold B. Mapping and quantifying mammalian transcriptomes by RNA-Seq. *Nat Methods*. 2008;5(7):621-628.
10. Robinson MD, Oshlack A. A scaling normalization method for differential expression analysis of RNA-seq data. *Genome Biol*. 2010;11(3):R25.

Figure S1

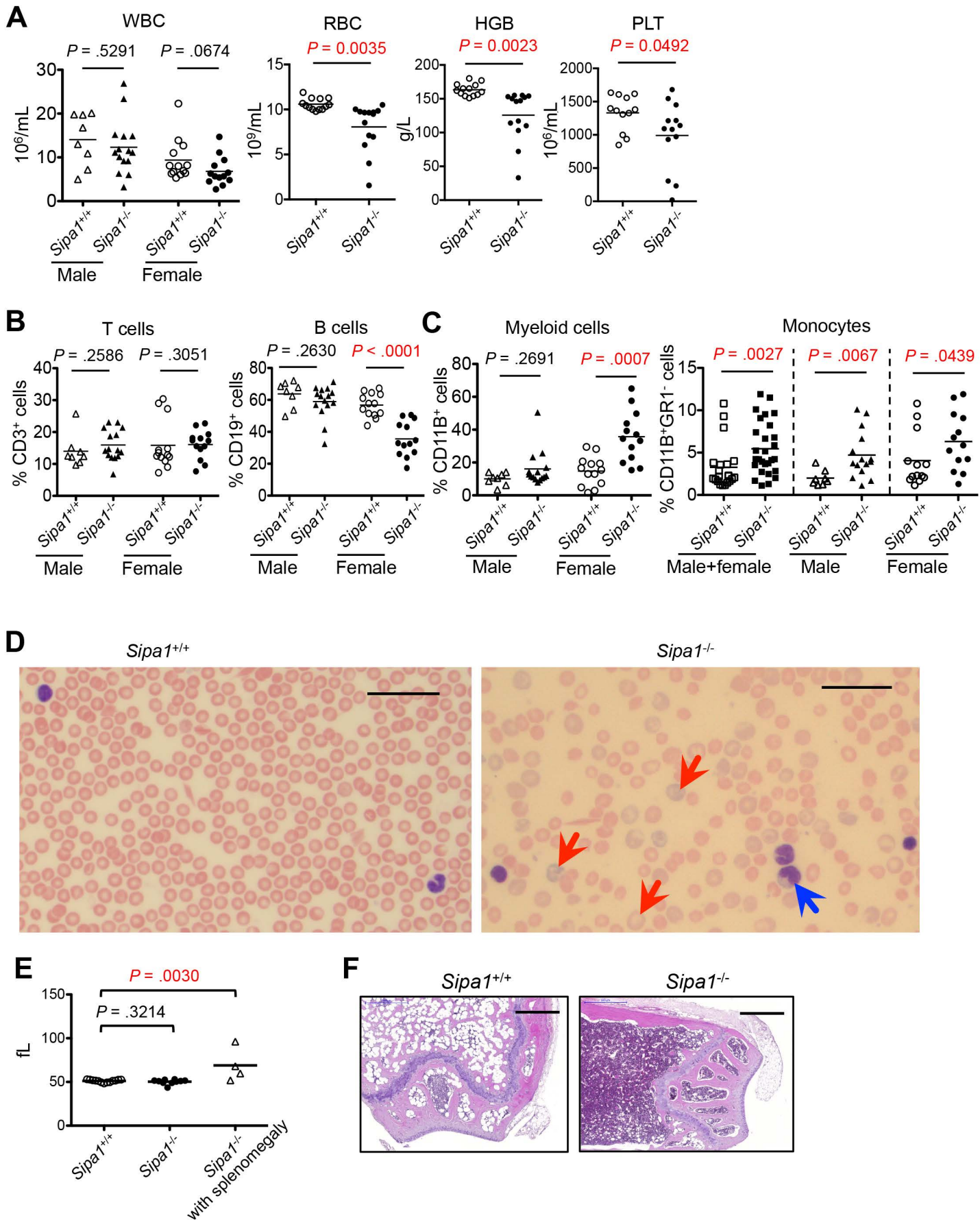
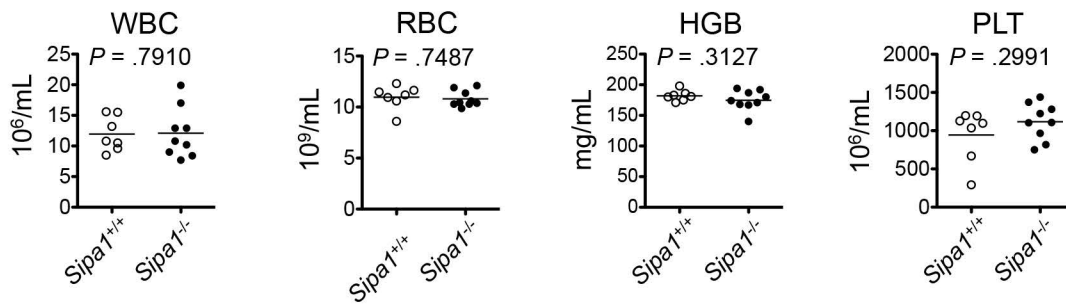
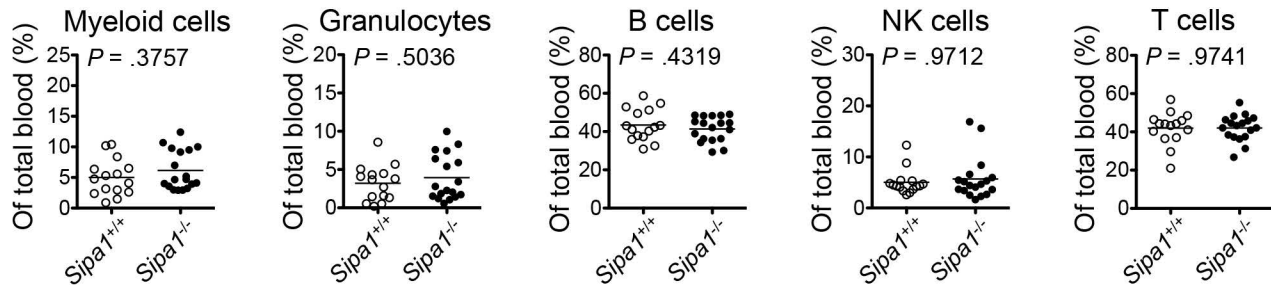


Figure S2

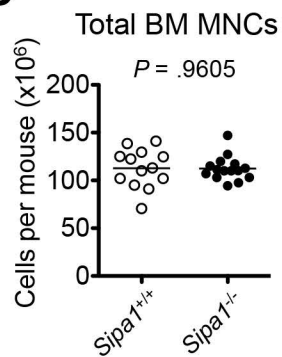
A



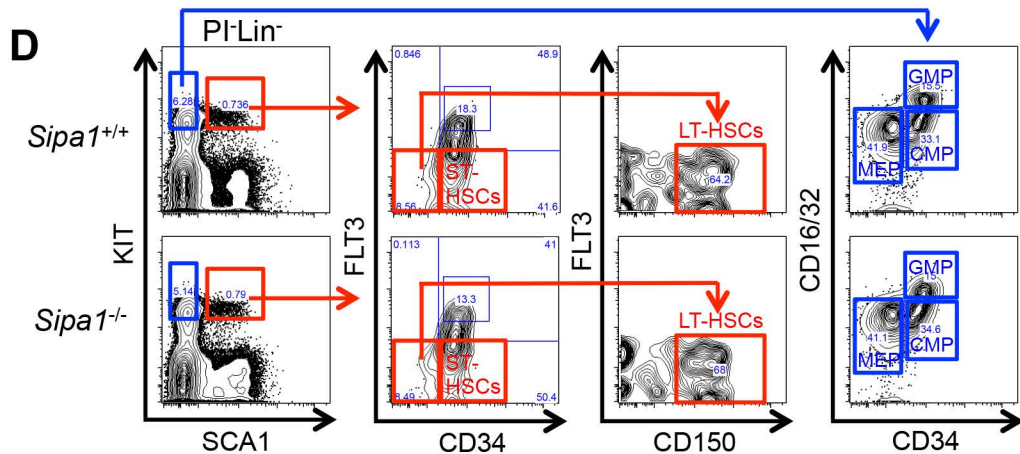
B



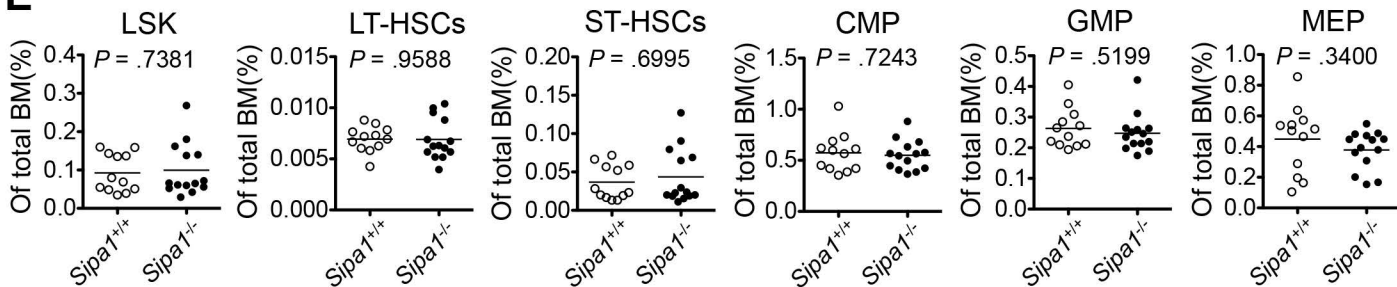
C



D



E



F

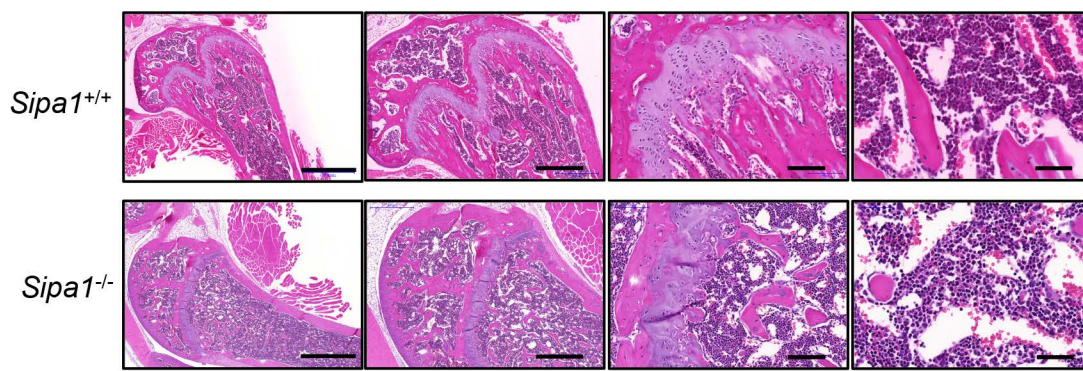
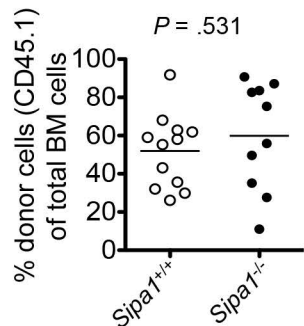
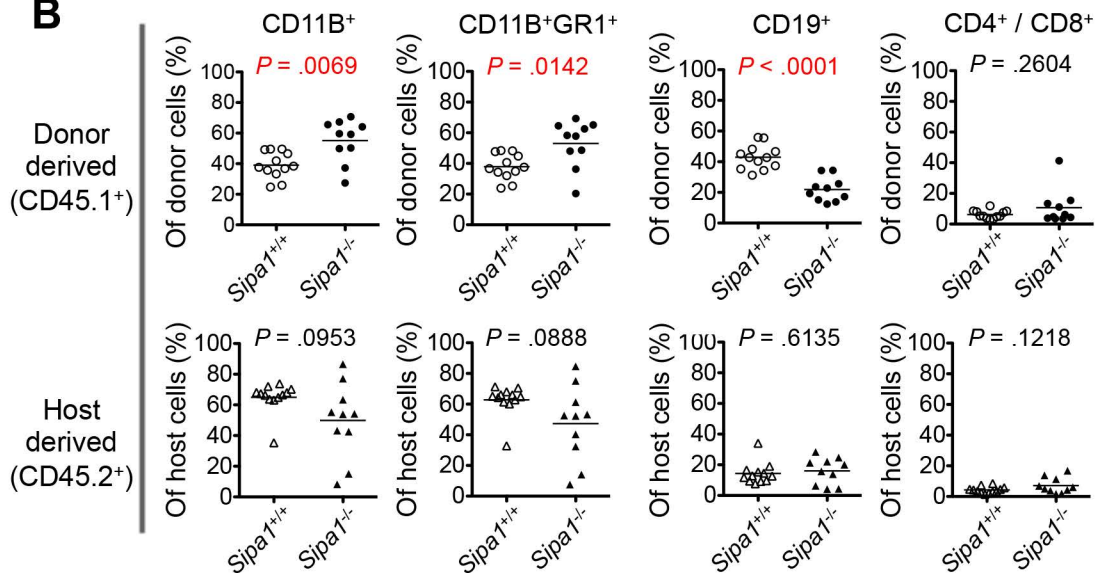


Figure S3

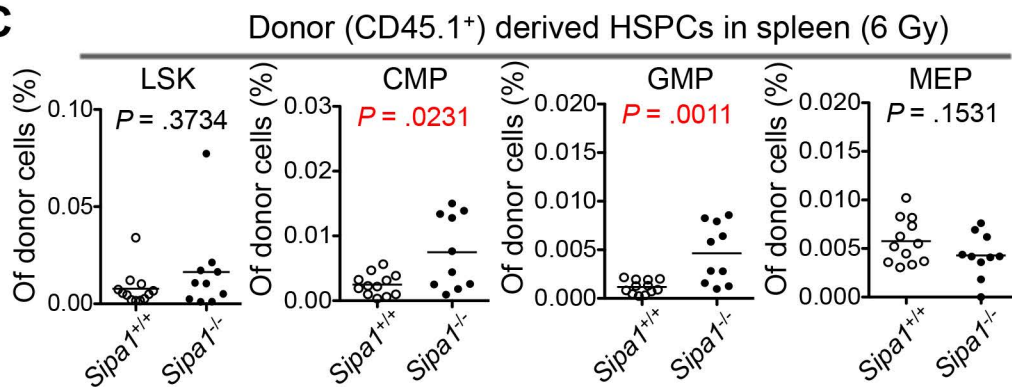
A



B



C



D

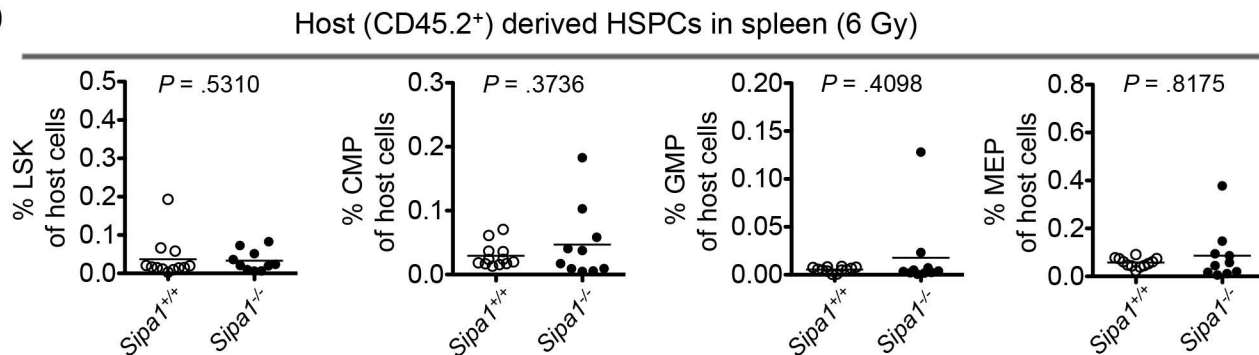


Figure S4

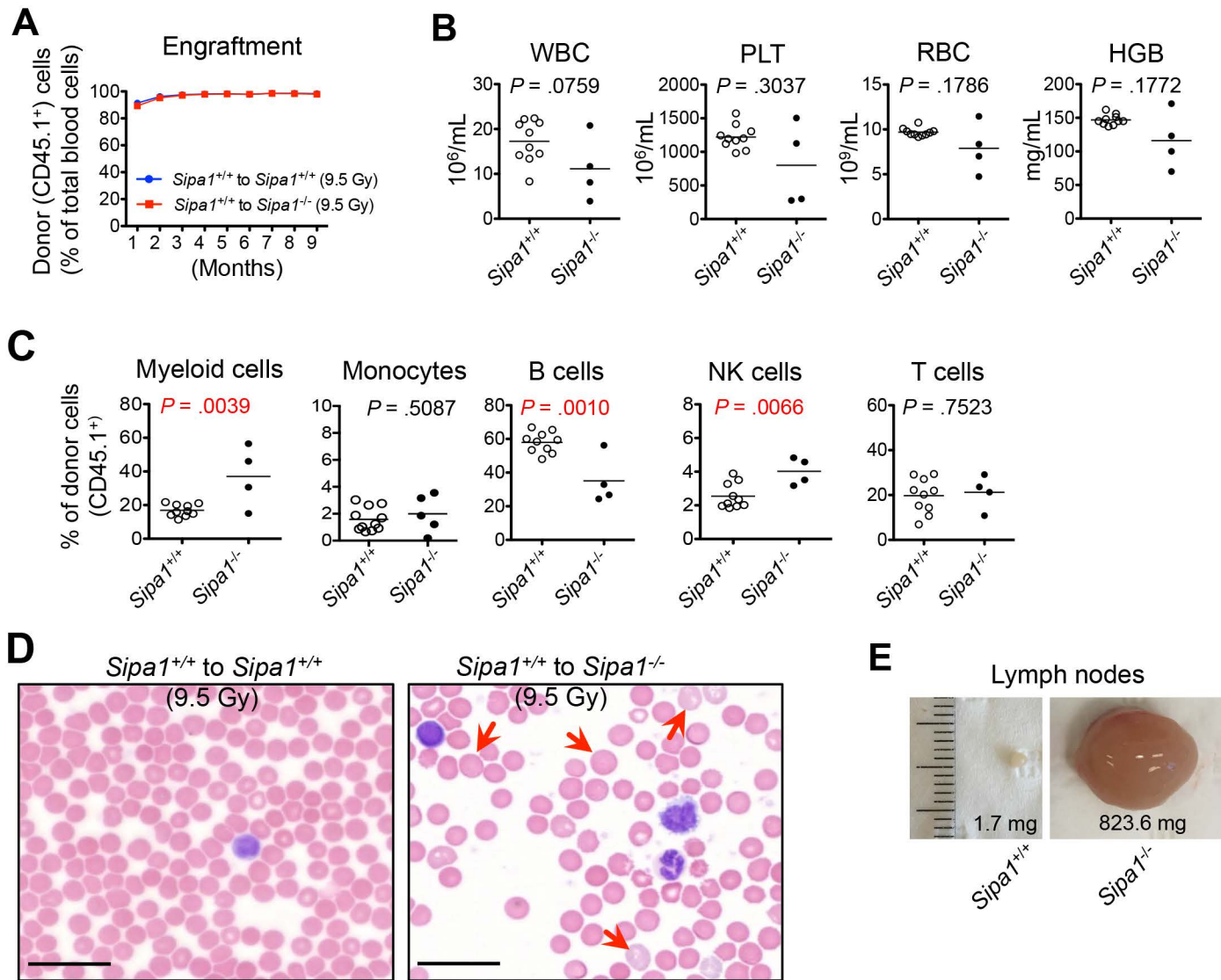


Figure S5

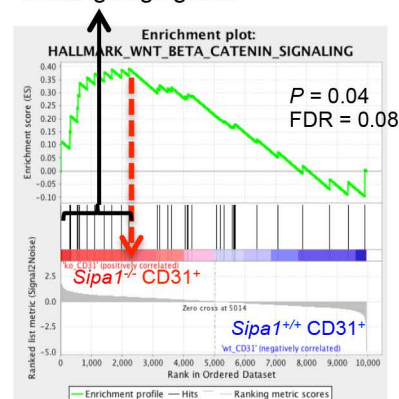
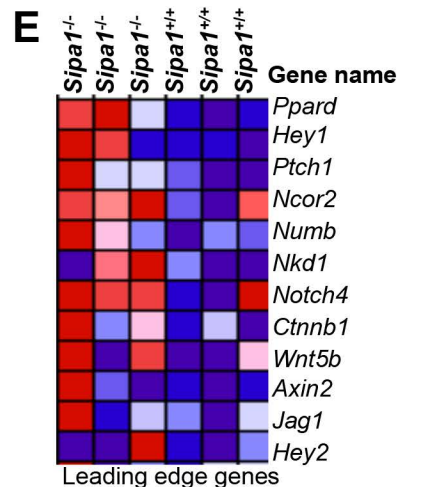
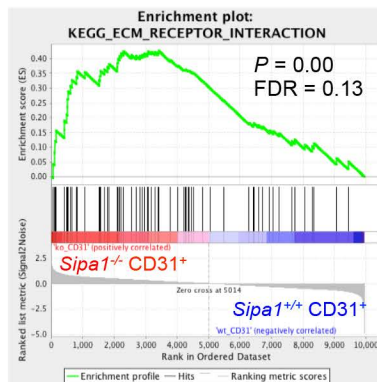
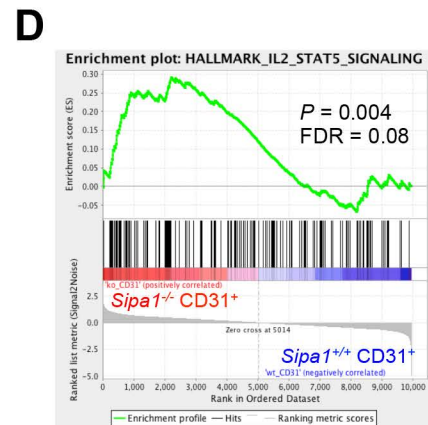
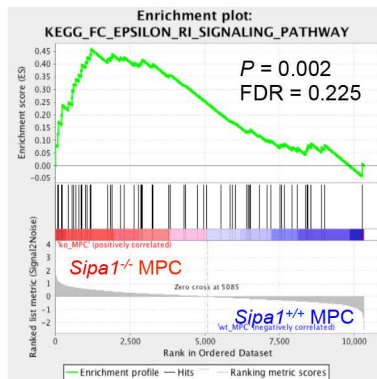
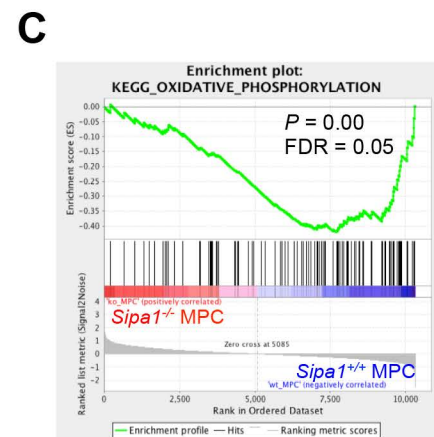
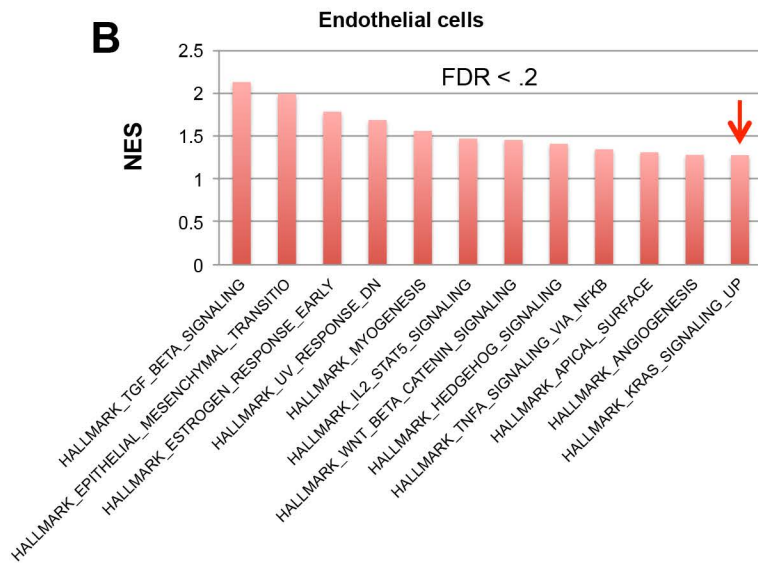
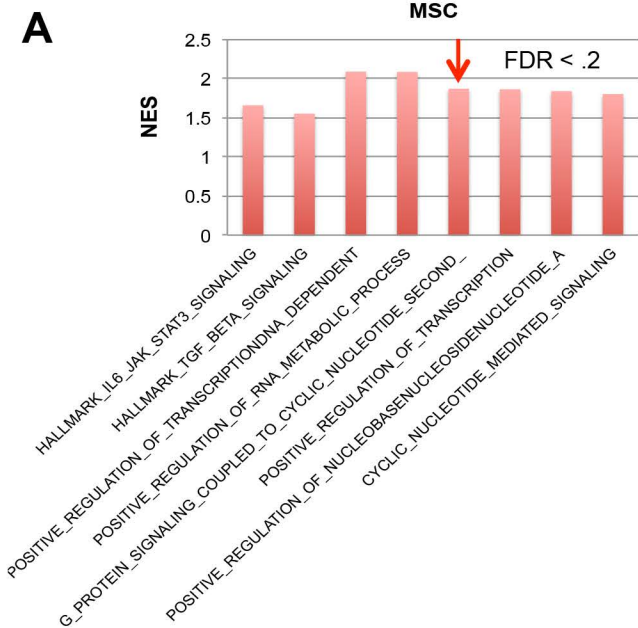
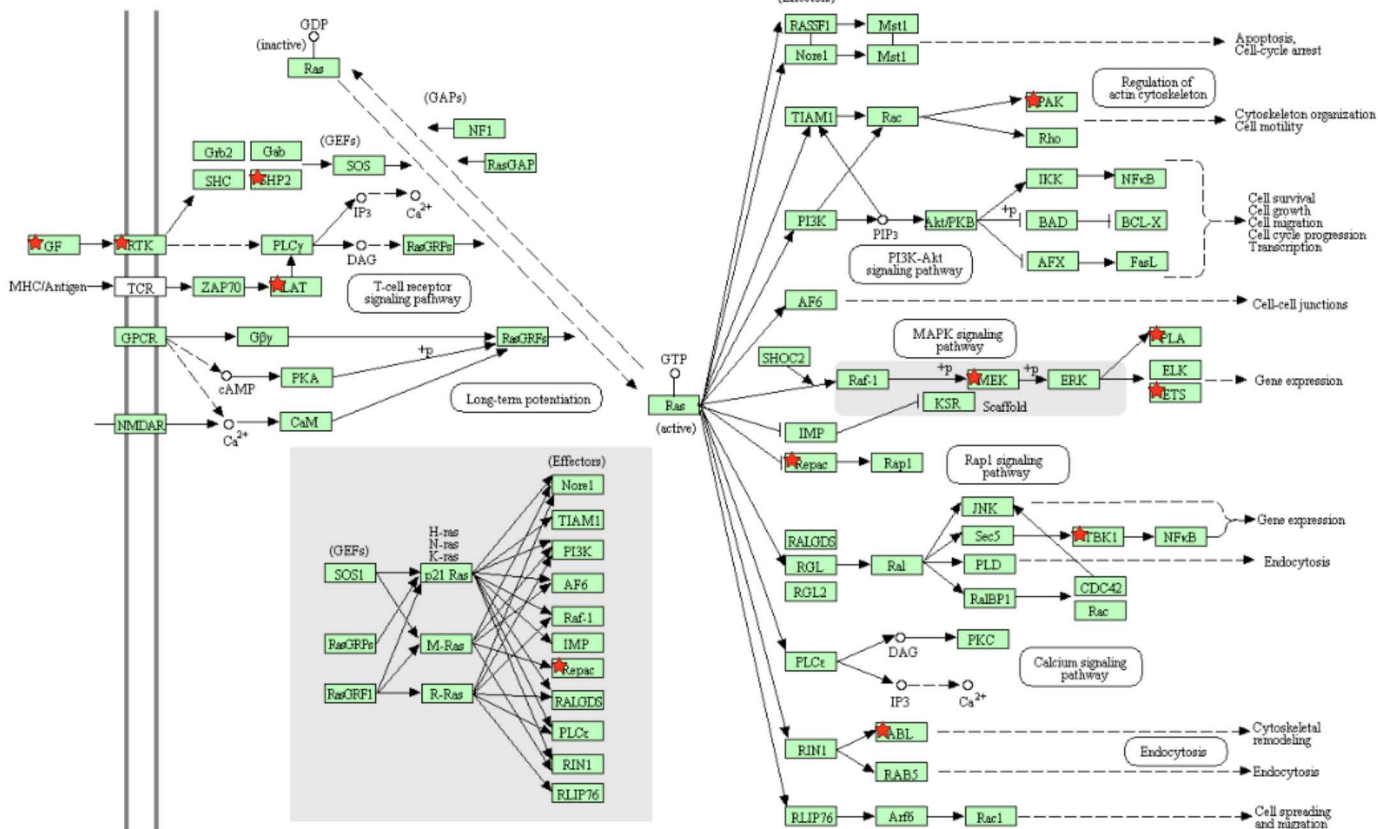


Figure S6

RAS SIGNALING PATHWAY



RAP1 SIGNALING PATHWAY

